In-plane anisotropy in BSCCO superconducting tapes: transport and magnetometric criteria

A. S. García-Gordillo[1], C. F. Sánchez-Valdés[2], J. L. Sánchez-Llamazares[3], E. Altshuler[1*]

*Corresponding author: ealtshuler@fisica.uh.cu

[1] Superconductivity Laboratory and Group of Complex Systems and Statistical Physics,
Physics Faculty-IMRE, University of Havana, 10400 Havana, Cuba.
[2] División Multidisciplinaria, Ciudad Universitaria,
Universidad Autónoma de Ciudad Juárez (UACJ), 32579 Ciudad Juárez, Chihuahua, México.
[3] División de Materiales Avanzados, Instituto Potosino de Investigación
Científica y Tecnológica A.C., 78216 San Luis Potosí, SLP, México.

Here, the anisotropy between the longitudinal and transverse directions of multi-filamentary $Bi_2Sr_2Ca_2Cu_3O_{10+x}$ tapes ("in plane" anisotropy) is studied by transport and magnetization measurements. By minimally manipulating experimental data, we quantify it using one number associated with transport measurements, and two numbers based on magnetization curves. We propose that the simplest and most reliable number is that based on the magnetization loop width. We propose that the best way to evaluate the in-plane anisotropy is to measure the vertical width of the M vs. H loop, where H is applied along two mutually perpendicular directions lying on the wide face of the tape.

Keywords: Superconducting wires, fibers and tapes, 84.71.Mn; Magnetic properties, 74.25.Ha; Superconductor transport properties, transport processes in superconductors, 74.25.F-

I. INTRODUCTION

From ceramic superconductors [1–6] to tapes [7–9], coated superconductors [10, 11] and films [12–14], the effects of inhomogeneities on superconducting properties have been systematically studied in the last decades. The effects of extended defects on the supercurrents along the longitudinal direction have been well studied for tapes and coated conductors [15, 16]. Despite the fact that the in-plane transverse direction constitutes the only available path for the current in the presence of lateral cracks [19, 20], transverse current transport has been rarely studied in superconducting tapes [17, 18].

Magneto-optics has been used to investigate the transverse critical current of Ag-sheated multi-filamentary $Bi_2Sr_2Ca_2Cu_3O_{10+x}$ tapes [21, 22], showing moderate anisotropy between the longitudinal and transverse dissipations only at low temperatures. Later on, we have found and characterized the anisotropy in the dissipation associated with *transport* currents in the longitudinal *vs.* transverse directions for similar tapes [23–26].

Finding new and simpler ways to determine the "in-plane" anisotropy in multi-filamentary BSCCO tapes can be very helpful. Here, the anisotropy between the longitudinal and transverse directions of multi-filamentary superconducting tapes of $Bi_2Sr_2Ca_2Cu_3O_{10+x}$ is studied by means of transport and magnetization measurements. Two different criteria based on magnetization curves and other associated with transport measurements were defined, resulting in adimensional numbers associated with the anisotropy in the plane of the tape. The pros and cons of each criterion are discussed.

II. EXPERIMENTAL DETAILS

The original tape was prepared by the powder-in-tube method [27]. It is 4.32 mm wide and 0.23 mm thick; and has an engineering critical current of 65 A at 77 K, equivalent to a critical current density of 6540 $A\ cm^{-2}$. The tape contains 61 filaments and each one is 0.3-0.4 mm wide and near 25 μm thick (see Fig. 1(a)).

Transport measurements were performed using the four-probe technique on narrow bridges cut from the tape in the longitudinal and transverse directions as shown in Fig. 1(b). Then, we were able to study separately the conduction along the longitudinal and transverse directions.

To obtain the M vs. μ_0H curves, the magnetization of an almost squared slice of tape of approximately 4×4 mm^2 was measured using the Vibrating Sample Magnetometry (VSM) option of a Dynacool Quantum Design PPMS system with a maximum magnetic field of $9T$. The sample was glued to the VSM sample holder using
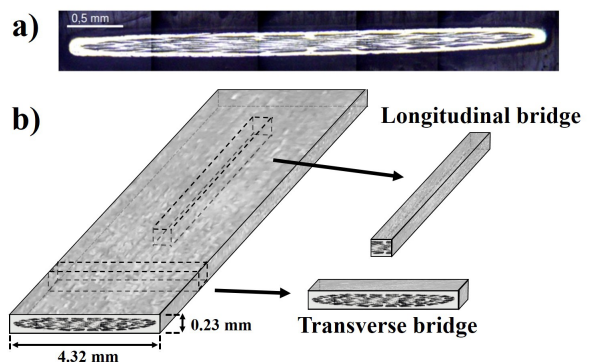

FIG. 1: Tape and bridges. (a) Cross-section of the BSCCO multi-filamentary tape. (b) Sketch showing the extraction of longitudinal and transverse bridges.
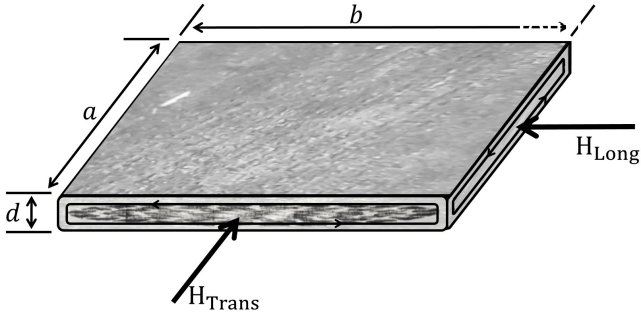
FIG. 2: Sketch of a BSCCO sample used for magnetometric measurements. The "Long" and "Trans" configurations are illustrated by the orientation of the magnetic field. The shielding currents associated with applied fields are represented by closed loops with arrows indicating the current direction.

GE-7031 varnish.

A sketch of the sample, including the configurations set in the magnetometer are shown in Fig. 2. Notice that the shielding currents associated with the "Long" configuration flow along the longitudinal and vertical directions, and the shielding currents associated with the "Trans" configuration flow along the transverse and vertical directions. All measurements were done in the ZFC regime.

III. RESULTS AND DISCUSSION

A. Analysis of transport data

The I-V curves measured on the longitudinal and transverse bridges are the most direct way to obtain the critical current density. In this section we reanalyze raw data published in a previous paper by us [24].

If the standard electric field criterion of 1 $\mu V/cm$ is used to determine the critical current density values at different temperatures from the I-V curves reported in [24], the critical current density values extracted from the transverse direction would be virtually zero, making impossible the comparison between one direction and the other. This happens because in this direction the current cannot find a continuous superconducting path spanning from one voltage contact to the other, because of the silver matrix containing the filaments, so there is dissipation for any nonzero value of temperature and current.

Defining "onset" critical current densities (J_c^{on}) at electric field values sufficiently larger than 1 $\mu V/cm$ allows to evaluate the "in-plane" anisotropy in terms of the I-V curves. Let J_c^{onT} and J_c^{onL} be the onset critical current densities determined in the transverse and longitudinal bridges, respectively. The temperature dependence of the J_c^{onT}/J_c^{onL} ratio is shown in Fig. 3 for several values of electric field criteria in the range 0.004 $V/m-$ 0.1 V/m.

Fig. 3 shows that there is always anisotropy in the plane of the tape. The values of J_c^{onL} are larger than those of J_c^{onT} indicating better superconducting properties in the longitudinal direction than in the transverse one. The J_c^{onT}/J_c^{onL} ratio increases with temperature

for low electric field criteria, indicating an anisotropy decrease. For larger criteria it slightly decreases with temperature. The inset of Fig. 3 shows the anisotropy calculated as before, except for the fact that the transverse critical current was determined after subtracting the linear contribution of the Ag matrix from the I-V curves. As a result, all curves move up (i.e., less anisotropy is seen) and the anisotropy number depends less on the voltage criteria. The extrapolation of all the curves at high temperatures suggests the existence of anisotropy not only in the superconducting state but also in the normal state. It may have different causes. Firstly the cold working may have produced anisotropy in the Ag resistivity –that can be of the order of 5% [28]. Secondly, the anisotropy may be related to the morphology of the tape: the different configurations of silver paths in the longitudinal and transverse directions make the current flow along a larger path in the transverse direction, so the effective resistivities are different in both directions in the normal state. Finally, the nature of superconducting vortices and their pinning are different for both configurations.

B. Magnetization measurements

To further investigate the anisotropy in the superconducting BSCCO tape, two different criteria based on magnetization curves were defined. The first criterion is based on the magnetization loops widths ΔM at zero applied field and the other is related to the full penetration fields H_p' [29] measured in the "Long" and "Trans" configurations of the applied field. In order to illustrate how this information is extracted from the magnetization loops, Fig. 4(a,b) presents a sketch of two magnetization loops as measured in the "Long" (black curve) and "Trans" (red curve) configurations at a given tempera-
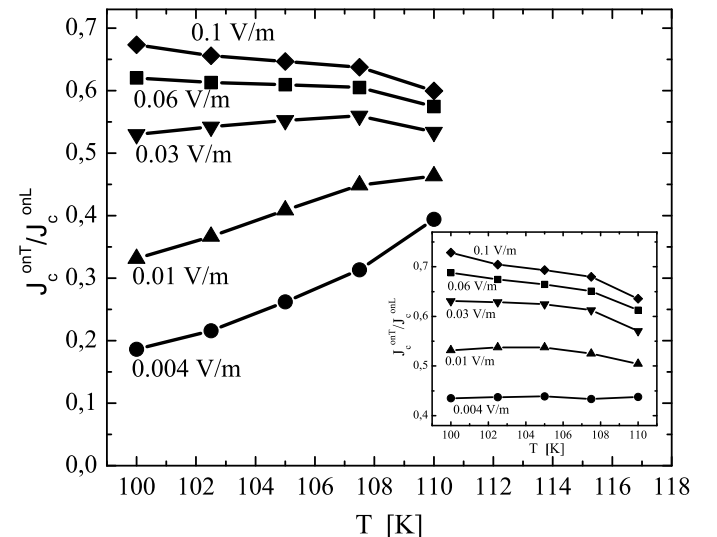

FIG. 3: Anisotropy of the onset critical current density. Temperature dependence of the J_c^{onT}/J_c^{onL} ratio for different values of electric field criteria. The inset shows the anisotropy calculated after subtracting the linear slope associated with the Ag matrix from the transverse I-V curves.

ture. The minimum observed in the initial magnetization curves corresponds to the value of the full penetration field. We are assuming that it is given by $H_p' = H_{c1} + H_p$, where H_{c1} is the first critical field of the sample, and H_p is the "pure" full penetration field as defined by Bean [29] (while Kim's model is, in principle, a more accurate choice to describe our magnetization loops, we will use Bean's model for the sake of simplicity). Fig. 4(a) also illustrates how ΔM is determined. It should be noted noted that both H_{c1} and H_p' are effective values associated with the whole composite.

The hysteresis loops for the "Long" and "Trans" configurations were measured at 70 K, 80 K, 90 K and 100 K. In Fig. 4(c,e) the magnetization loops for two values of temperature in both configurations are shown. Notice that no diamagnetic backgrounds were subtracted from the graphs, since they were negligible (if that contribution is significant, it should be eliminated, as illustrated in [30]). It is not difficult to note the differences between the magnetization loops widths for the "Long" and "Trans" configurations. The displacements of the minima of the initial magnetization curves (H_p') for all temperatures are not that evident from Fig. 4(d,f), but
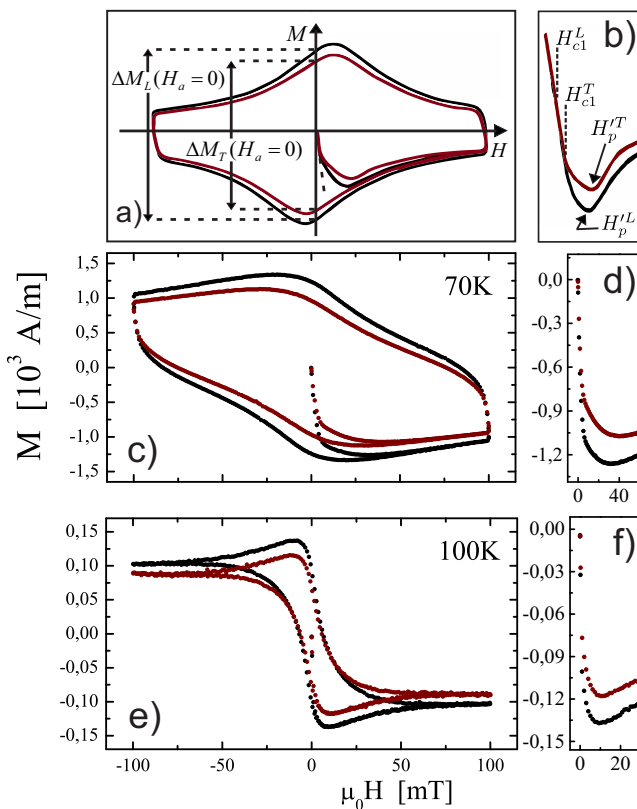
they can be easily verified through the first derivative of the magnetization.

Fig. 5 shows that the anisotropy associated with the width of the loops is within the range $0.75 \leq \Delta M^T / \Delta M^L \leq 0.78$, and that it does not depend substantially on the temperature. The connection of this parameter with the anisotropy in the current distribution inside the multi-filamentary tape is not straightforward. Modifications of Bean's model to account for the presence of anisotropic critical currents plus demagnetization effects have been thoroughly treated in the literature, especially for the case of HTc crystals, where critical current densities are much bigger along the ab-planes than along the c-axis, while demagnetizations are typically much smaller for magnetic fields applied along the ab-plane than for those along the c-axis (a,b cannot be confused with sample dimensions shown in Fig. 2) [31–33]. In our case, there are further complications: instead of crystals, we have filaments formed by a collection of inter-connected crystals, and the filaments themselves are arranged anisotropically inside the tape, so the whole composite eventually displays granular-like behaviour and anisotropy at different levels [34].

It is instructive to illustrate the complexity of the situation by applying to our data a version of Bean's model that assumes anisotropic currents, but no demagnetization –which should not be very important in our case, since we measure ΔM by applying relatively large magnetic fields parallel to the wide face of the samples. Gyorgy et $al.$ [31] analyze the case of a superconducting slab of rectangular cross section of dimensions l and t with critical currents J_{c1} and J_{c2} flowing parallel to l and t, respectively. If we translate their results to our case (Fig. 2) assuming $a = b$, we get $\Delta M^T / \Delta M^L = (J_c^T / J_c^L)[1 - (dJ_c^T)/(3aJ_c^P)]/[1 - (dJ_c^L)/(3aJ_c^P)]$ if $J_c^T / J_c^P < a/d$ and $J_c^L / J_c^P < a/d$, while $\Delta M^T / \Delta M^L = [1 - (aJ_c^P)/(3dJ_c^T)]/[1 - (aJ_c^P)/(3dJ_c^L)]$ if $J_c^T / J_c^P > a/d$ and $J_c^L / J_c^P > a/d$. In the previous equations, J_c^L and J_c^T are the effective critical current densities along the longitudinal and transverse directions

FIG. 4: Magnetization loops. (a) Sketch illustrating the main relevant parameters in the configurations "Long" (black curve) and "Trans" (red curve). (b) Initial magnetization curves sketch illustrating H_{c1}^T, H_{c1}^L, $H_p'^T$ and $H_p'^L$. (c) Magnetization loops at 70 K. (d) Initial magnetization curves at 70 K. (e) Magnetization loops at 100 K. (f) Initial magnetization curves at 100 K.
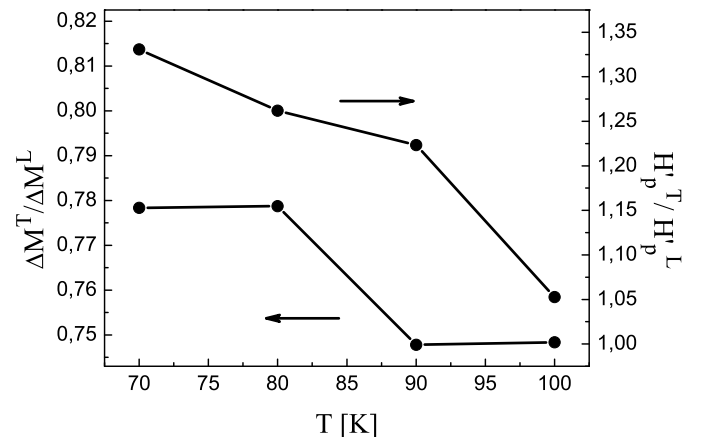

FIG. 5: Temperature evolution of the two anisotropy parameters based on magnetization curves (see text).

of the tape respectively, and J_c^P is the analogous value along the direction perpendicular to the wide face of the tape. In order to understand the relation of the measured anisotropy in the width of the magnetization loops with the anisotropy between the in-plane critical current densities, a reasonable strategy would be to measure the transport critical current density perpendicular to the wide plane of the tape, so we are able to fully understand the previous equations. It will be the subject of future work.

Let us now explore a second criterium to evaluate in-plane anisotropy based on the magnetization loops: the comparison of the magnetization minima H_p'. We are assuming that $H_p' = H_{c1} + H_p$, where H_{c1} is the first critical field of the sample, and H_p is the "pure" full penetration field as defined by the critical state model [29]. Looking at Fig. 4 we can see the differences of the minima in the "Long" and "Trans" configurations. Fig. 5 shows the temperature dependence of the anisotropy expressed as the ratio between the transverse and longitudinal full penetration fields, $H_p'^T/H_p'^L$. If we follow the same rationale as in the case of the anisotropy in the magnetization loop widths, the anisotropy of the magnetization minima would indicate stronger superconductivity along the transverse direction, which seems to contradict the previous measurements. We speculate that the observed anisotropy in $H_p'^T/H_p'^L$ could be provoked by the effect on H_{c1}^T and H_{c1}^L of the demagnetization associated with the different configurations of superconducting filaments that the magnetic field finds when applied along the longitudinal and transverse directions. Notice that demagnetization effects are more important at low fields, so we did not considered them when discussing the former anisotropy criterion based on the width of the magnetization loops.

IV. CONCLUSIONS

We have defined a variety of criteria –based on minimal manipulations of transport and magnetic measurements– to quantify the "in plane" anisotropy in a BSCCO multifilamentary tape. Under all criteria, anisotropy has been found.

We propose that the simplest, most practical and reliable criterion to evaluate the in-plane anisotropy is the comparison of the hysteresis loop widths applying the magnetic field in two mutually perpendicular directions parallel to the plane of the tape. Notice that this kind of measurement only requires a 90° turn in a magnetometer, and is very robust since it does not require an *ad hoc* rule, like the establishment of electric field thresholds used in the transport measurements.

Further studies are needed to understand in detail how the precise morphology of the tapes influence the in-plane anisotropy.

[1] J. R. Clem *Physica C* **153-155 (part1)**, 50 (1988).

[2] E. Altshuler, J. Musa, J. Barroso, A.R.R. Papa, V. Venegas *Cryogenics* **33 (3)**, 308-313 (1993).

[3] E. Altshuler, R. Cobas, A. J. Batista-Leyva, C. Noda, L. E. Flores, C. Martínez and M.T.D. Orlando *Phys. Rev. B* **60**, 3673 (1999).

[4] A. J. Batista-Leyva, R. Cobas, E., M. T. D. Orlando and E. Altshuler *Supercond. Sci. Tecnol.* **16**, 857 (2003).

[5] S. Recuero, N. Andrés, J. Lobera, M. P. Arroyo, L. A. Angurel and F. Lera *Meas. Sci. Technol.* **16**, 1030 (2005).

[6] W. Treimer, O. Ebrahimi and N. Karakas *Appl. Phys. Lett.* **101**, 162603 (2012).

[7] K. Ogawa and K. Osamura *Phys. Rev. B* **67**, 184509 (2003).

[8] M. Zhang, J. Kvitkovic, J. H. Kim, C. H. Kim, S. V. Pamidi and T. A. Coombs *Appl. Phys. Lett.* **101**, 102602 (2012).

[9] W. Chen, H. Zhang, Y. Chen, X. Yang, Y. Zhang and Y. Zhao *Cryogenics* **94**, 1-4 (2018).

[10] S. Trommler, R. Hühne, E. Reich, K. Ida, S. Haidndl, V. Matias, L. Schultz and B. Holzapfel *Appl. Phys. Lett.* **100**, 1226602 (2012).

[11] D. Colangelo and B. Dutoit *Supercond. Sci. Technol.* **25**, 1 (2012).

[12] J. Hua, Z. L. Xiao, D. Rosenmann, I. Beloborodov, U. Welp, W. K. Kwok and G. W. Crabtree. *Appl. Phys. Lett.* **90**, 072507 (2007).

[13] L. Del Río, E. Altshuler, S. Niratisairak, O. Haugen, T. H. Johansen, B. A. Davidson, G. Testa and E. Sarnelli *Supercond. Sci. Technol.* **23**, 085005 (2010).

[14] T. Horide and K. Matsumoto *Appl. Phys. Lett.* **101**, 112604 (2012).

[15] X. Y. Cai, A. Polyanskii, Q. Li, Jr. G. N. Riley and D. C. Larbalestier *Nature* **392**, 906 (1998).

[16] D. C. van der Laan, M. Dhallé, H. J. N. van Eck, A. Metz, B. ten Haken, H. H. J. ten Kate, L. M. Naveira, M. W. Davidson and J. Schwartz *Appl. Phys. Lett.* **86**, 032512 (2005).

[17] A. S. García-Gordillo, A. Borroto and E. Altshuler *Rev. Cub. Fis.* **31**, 96 (2014).

[18] A. S. García-Gordillo, A. Reyes and E. Altshuler *Rev. Cub. Fis.* **36**, 73 (2019).

[19] K. Isozaki, T. Noda, S. Iwasaki, R. Honzawa, T. Ojima, T. Takao, Y. Iida, T. Ogino y O. Tsukamoto *IEEE Trans-*

actions on Applied Superconductivity **23**, 6601504 (2012).

[20] H. Akiyama, Y. Tsuchiya, S. Pyon and T. Tamegai *Physica C* **504**, 65 (2014).

[21] M. R. Koblischka, T. H. Johansen, B. H. Larsen, N. H. Andersen, H. Wu, P. Skov-Hansen, M. Bentzon and P. Vase *Physica C* **341-348**, 2583 (2000).

[22] A. V. Bobyl, D. V. Shantsev, T. H. Johansen, M. Baziljevich, Y. M. Galperin and M. E. Gaevski *Supercond. Sci. Technol.* **13**, 183 (2000).

[23] C. F. Sánchez-Valdés, C. Pérez-Penichet, C. Noda, M. Arronte, A. J. Batista-Leyva, Ø Haugen, T. H.Johansen, Z. Han and E. Altshuler *J. Mag. Mag. Mat.* **316**, 930 (2007).

[24] A. Borroto, L. Del Río, E. Altshuler, M. Arronte, P. Mikheenko, A. Qviller and T. H. Johansen *Supercond. Sci. Technol.* **26**, 115004 (2013).

[25] A. Borroto, L. Del Río, M. Arronte, T. H. Johansen and E. Altshuler *Appl. Phys. Lett.* **105**, 202604 (2014).

[26] A. Borroto, A. S. García-Gordillo, L. Del Río, M. Arronte, and E. Altshuler *Supercond. Sci. Technol.* **28**, 075008 (2015).

[27] P. Vase, P. Skov-Hansen, Z. Han, H. F. Poulsen and T. Frello, European Conference on Applied Superconductivity, The Netherlands, 1997.

[28] C. W. Berghout *Physica* **18(11)**, 978-979 (1952).

[29] Ch. P. Bean *Rev. Mod. Phys.* **36**, 31 (1964).

[30] D. A. Balaev, D. M. Gokhfeld, S. I. Popkov, K. A. Shaikhutdinov, L. A. Klinkova, L. N. Zherikhina, and A. M. Tsvokhrebov *JETP* **118**, 104 (2014).

[31] E. M. Gyorgy, R. B. Van Dover, K. A. Jackson, L.F. Schneemeyer and J. V. Waszczak *Appl. Phys. Lett.* **55**, 283 (1989).

[32] F. M. Sauerzopf, H. P. Wiesinger and H. W. Weber *Cryogenics* **30 (7)**, 650-655 (1990).

[33] Th. Schuster, H. Kuhn, E. H. Brandt and S. Klaumünzer *Phys. Rev. B* **56**, 3413 (1997).

[34] M. R. Koblischka, L. Púst, A. Galkin and P. Nálevka *Appl. Phys. Lett.* **70**, 514 (1997).